Improvement on peak-to-trough ratio of sampled fiber Bragg gratings with multiple phase shifts

Bin Xie (谢 滨), Wei Pan (潘 炜), Bin Luo (罗 斌), and Xihua Zou (邹喜华)

School of Information Science and Technology, Southwest Jiaotong University, Chengdu 610031

Received July 17, 2007

Via a cascaded structure, the peak-to-trough ratio is considerably improved for sampled fiber Bragg gratings (SFBGs) based on multiple-phase-shift (MPS) technique. This cascaded filter is composed of two identical SFBGs which are inserted with the increasing or decreasing arrangement of phase shifts. With this inverse arrangement of MPS in grating design, the phase fluctuation of individual SFBG can be compensated, and as a result an excellent phase matching condition is realized. In this way, the peak-to-trough ratio in reflection spectra is improved from 6 to 12 dB when multiplication factor $m = 4$, and from 5 dB to 10 dB when $m = 8$.

OCIS codes: 050.2770, 050.5080, 060.2340.

Up to now, fiber Bragg gratings (FBGs) have already evolved into essential optical devices for optical communication and sensing systems. In the big family of FBGs, in particular, sampled FBGs (SFBGs) exhibit comb-like reflection (or transmission) spectra, which result from periodic amplitude sampling[1−3], phase sampling[4,5], multiple-phase-shift (MPS) technique[6], or chirp-induced Talbot effect[7−9]. These comb-like spectra are more attractive for multichannel operation, especially for multichannel multiplexers-demultiplexers[10], multichannel dispersion compensators[4,5], and high channel-count comb filters[8,11,12].

In Ref. [6], the MPS technique has been proposed to densify the channel spacing of SFBGs. However, the peak-to-trough ratio (or interchannel sidelobes) of spectra is not good enough. To improve the peak-to-trough ratio, three-step apodization process or sinc-shaped sampling profile is adopted. These extra processes add to the complexity of manufacture to some extent. Meanwhile, Magné *et al.*[13] recently have introduced a cascaded configuration to eliminate the phase fluctuation of spectral Talbot effect. This cascaded configuration is able to suppress interchannel sidelobes remarkably, which is beneficial for improving the peak-to-trough ratio of MPS technique as well.

Therefore, so as to improve the peak-to-trough ratio with a relatively simple method, we introduce a cascaded grating design for MPS-based SFBGs. In detail, two identical SFBGs with MPS technique are concatenated in an inverse way via circulators. Because there is an excellent phase matching condition between the phases of two SFBGs, interchannel sidelobes are significantly suppressed and the peak-to-trough ratio is greatly enhanced even without extra apodization processes.

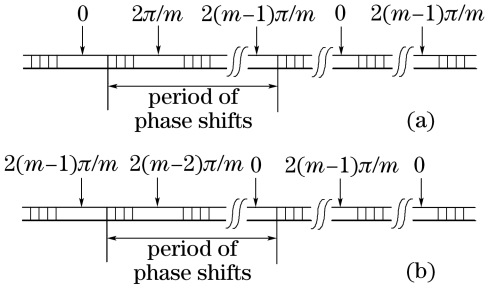

Fig. 1. Schematic diagram of SFBGs with (a) increasing and (b) decreasing arrangement of MPS.

As for MPS-based SFBGs, the schematic diagram is shown in Fig. 1. Besides the amplitude sampling, MPS technique also introduces phase shifts into FBG sections. These phase shifts $\phi(k)$ between kth and $(k+1)$th sections can be arranged in an increasing or decreasing way, as shown in Figs. 1(a) and (b). Mathematically, $\phi(k)$ is expressed as

$$\phi_1(k) = \frac{2\pi}{m} \times [(k-1) \bmod m],\ k = 1, 2, 3, \cdots, N, \quad (1a)$$

$$\phi_2(k) = \frac{2\pi}{m} \times [(N-k) \bmod m],\ k = 1, 2, 3, \cdots, N, \quad (1b)$$

where m is the multiplication factor of MPS and N is the total number of sampling period. Obviously, Eq. (1a) shows a rising arrangement, corresponding to SFBG-1, while Eq. (1b) corresponding to SFBG-2 is a decreasing arrangement. Here, the subscripts 1 and 2 refer to SFBG-1 and SFBG-2, respectively. Except for the arrangement difference, other corresponding parameters of SFBG-1 and SFBG-2 are identical. In other words, SFBG-2 is the very inverse form of SFBG-1. This difference in arrangement of phase shifts will play a decisive role in the cascaded design.

When it comes to filtering performance, both SFBGs are with the same channel bandwidth and channel spacing, and the channel spacing can be given by

$$\Delta f_{\mathrm{mps}} = \frac{\Delta f}{m} = \frac{c}{2mnP}, \quad (2)$$

where c is the velocity of light in vacuum, n is the effective refractive index, $\Delta f = c/(2nP)$ is the nominal channel spacing (spacing of initial SFBG without MPS), and P is the sampling period. From Eq. (2), it is easy to know that the channel spacing is multiplied by m times

via the MPS technique.

For further investigation, we have to turn to Fourier theory. In this way, each reflection channel in the spectrum can be weighted by a complex factor[6]

$$S_1(m,p) = \sum_{i=1}^{2m} \exp j\left[\pi\left(p+i-1\right)/m\right] i$$

$$= |S_1(m,p)| \exp(j\varphi_1(m,p)), \tag{3a}$$

$$S_2(m,p) = \sum_{i=1}^{2m} \exp j\left[\pi\left(p-i-1\right)/m\right] i$$

$$= |S_2(m,p)| \exp(j\varphi_2(m,p)), \tag{3b}$$

where $p = 0, \pm 1, \pm 2, \cdots$ identifies the order of the wavelength channel and $j = \sqrt{-1}$. For respective MPS-based SFBG, unwanted interchannel sidelobes would deteriorate the output performance of SFBG and the peak-to-trough ratio of the filter is relatively low. Consequently, extra apodization processes are always used to improve the performance of such devices.

To overcome the problem mentioned above, we introduce a cascaded grating design for MPS technique. As shown in Fig. 2, two three-port circulators are used to connect SFBG-1 and SFBG-2. P_{in} and P_{out} refer to the input and output optical power of the cascaded design filter, respectively.

To demonstrate the principle of this cascaded design, we have to numerically analyze phase factor of the cascaded design. Under this design, the phase condition of the cascaded SFBGs $\Phi(m,p)$ can be expressed as

$$\Phi(m,p) = \varphi_1(m,p) + \varphi_2(m,p). \tag{4}$$

The respective phases of SFBG-1, SFBG-2 and the cascaded filter are numerically shown in Fig. 3. Each SFBG has a relatively low peak-to-trough ratio resulting from the phase fluctuation between the adjacent channels. Although with the same sampling function and spectral densification factor, we can see from Fig. 3 that the corresponding phase function of the cascaded comb filter satisfies proper phase matching condition $\Phi(m,p) = 2K\pi$, where K is an arbitrary integer number. Although a few channels do not properly satisfy this condition, sidelobes can also be suppressed because of the phase differences from each SFBG. All this is due to the difference in the arrangement of phase shifts. Consequently, the phase fluctuation can be compensated to a low value in the cascaded design.

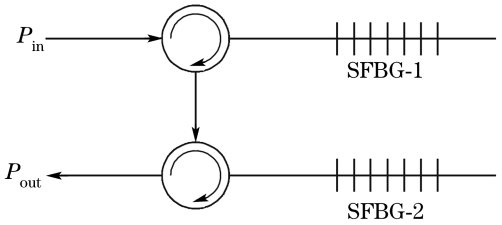

Fig. 2. Schematic diagram of the designed cascaded filter.

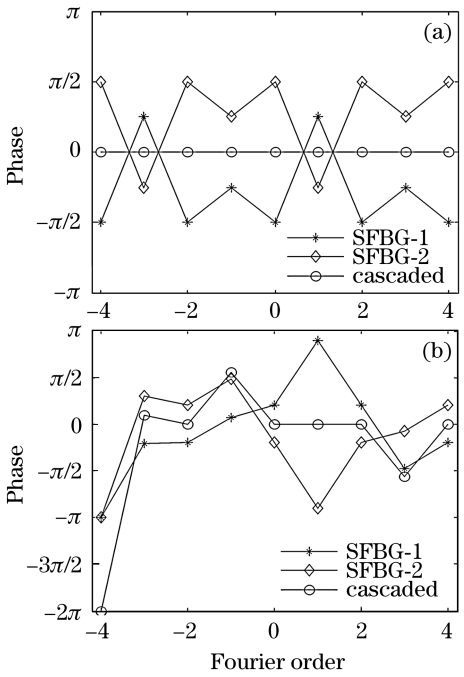

Fig. 3. Phase matching conditions with different Fourier orders. (a) $m = 2$; (b) $m = 5$.

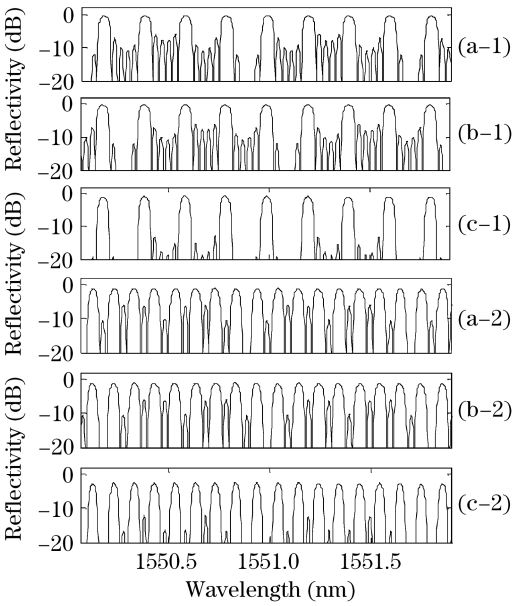

Fig. 4. Reflectivity of the MPS-based SFBG. (a) SFBG-1; (b) SFBG-2; (c) cascaded design. (1) $m = 4$, (2) $m = 8$.

In following simulations, we try to confirm our design above by transfer matrix method. The detailed parameters of the MPS-based SFBGs are as follows: $n = 1.485$, the Bragg period $\Lambda = 521.89$ nm, $P = 1.0$ mm, the sampling length $P_0 = 0.1$ mm, and $N = 24$. Figure 4 shows the reflectivity of MPS-based SFBGs when $m = 4$ and $m = 8$ (boundary condition of MPS constraints[6]), respectively. Both SFBG-1 and SFBG-2 provide similar periodic comb responses in amplitude, but exhibit a different interchannel phase variation due to the differences between the arrangements of phase shifts. When the two SFBGs are cascaded, the reflective spectrum is shown in Fig. 4(c). It is evident that the

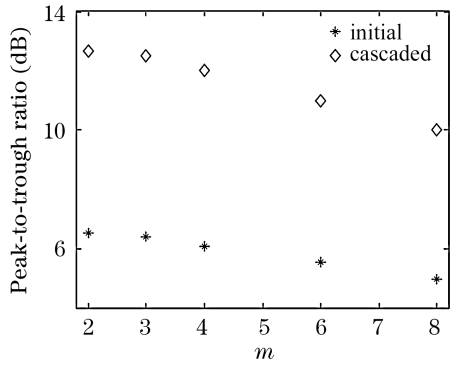

Fig. 5. Peak-to-trough ratio for different multiplication factor.

interchannel sidelobes are significantly suppressed and the peak-to-trough ratio of the cascaded configuration is greatly improved as expected. In detail, the interchannel sidelobes are suppressed from the initial value 6 dB to the improved value 12 dB when $m = 4$, and from 5 to 10 dB when $m = 8$. The reflectivity of each channel has reduced by only a low value (about 0.5 and 1 dB, respectively). Compared with the decrease of peak value, the improvement of peak-to-trough ratio is far more considerable in our design. Further, we also analyze the improvement on peak-to-trough ratio for different multiplication factor in Fig. 5, while keeping the rest of parameters unchanged. Clearly, it can be seen that with the increase of multiplication factor, both peak-to-trough ratio of single SFBG and that of cascaded filter decrease to a lower value, and the improvement of sidelobes suppression relatively weakens. This is mainly because the peak power drops while the sidelobes power increases with the increment of m, which is indicated in Ref. [6].

Furthermore, this cascaded design can be regarded as a unit. By arranging two or more such units with more circulators, the unwanted sidelobes can be suppressed further. For instance, the peak-to-trough ratio increases from nearly 12 dB ($M = 1$), 25 dB ($M = 2$), to 37 dB ($M = 3$), where M denotes the number of such units.

In conclusion, in order to enhance the peak-to-trough ratio, a counter-cascaded grating design has been proposed for MPS-based SFBGs. In this cascaded design, the phase fluctuation of individual SFBG is replaced by an excellent phase matching condition $\Phi(m, p) = 2K\pi$. Therefore, the peak-to-trough ratio of reflection spectra is considerably enhanced with this design. For example, the ratio increases from 6 to 12 dB when $m = 4$, and from 5 to 10 dB when $m = 8$. Moreover, by cascading two or more such units in series, sidelobes can be suppressed further.

This work was supported by the National Natural Science Foundation of China (No. 10174057, 90201011), the Key Project of Chinese Ministry of Education (No. 105148), and the Foundation of Key Laboratory of Optical Fiber Transmission and Communication Networks (No. KF2006). B. Xie's e-mail address is xiebin_swjtu@ 126.com.

References

1. B. Jia, Q. Sheng, D. Feng, and X. Dong, Chin. J. Lasers (in Chinese) **30**, 247 (2003).
2. X. Chen, Y. Luo, C. Fan, T. Wu, and S. Xie, IEEE Photon. Technol. Lett. **12,** 1013 (2000).
3. X. Zou, W. Pan, B. Luo, W. Zhang, and M. Wang, IEEE Photon. Technol. Lett. **18,** 529 (2006).
4. H. Lee and G. P. Agrawal, IEEE Photon. Technol. Lett. **15,** 1091 (2003).
5. X. Wang, C. Yu, Z. Yu, and Q. Wu, Chin. Opt. Lett. **2,** 190 (2004).
6. Y. Nasu and S. Yamashita, J. Lightwave Technol. **23,** 1808 (2005).
7. X. Zou, W. Pan, B. Luo, Z. Qin, M. Wang, and W. Zhang, IEEE Photon. Technol. Lett. **18,** 1371 (2006).
8. C. Wang, J. Azaña, and L. R. Chen, IEEE Photon. Technol. Lett. **16,** 1867 (2004).
9. X. Zou, W. Pan, B. Luo, M. Wang, and W. Zhang, Opt. Express **15,** 8812 (2007).
10. H. Cai, R. Huang, R. Qu, G. Chen, and Z. Fang, Chin. J. Lasers (in Chinese) **30,** 243 (2003).
11. X. Chen, C. Fan, Y. Luo, S. Xie, and S. Hu, IEEE Photon. Technol. Lett. **12,** 1501 (2000).
12. R. Qu, H. Ding, H. Zhao, Z. Fang, G. Ni, and H. Zhai, Acta Opt. Sin. (in Chinese) **19,** 226 (1999).
13. J. Magné, J. Azaña, S. LaRochelle, and L. R. Chen, IEEE Photon. Technol. Lett. **18,** 1958 (2006).